

Molecular identification and the effect of abiotic stress on bioactive metabolite production for endophytic *Bacillus* isolates from *Solanum nigrum*

Benedict Ndou

North-West University

Beauty-Ben Baloyi

North-West University

Nokufa Morrieson Mabona

North-West University

Matsobane Godfrey Tlou

Matsobane.T.Tlou@nwu.ac.za

North-West University

Research Article

Keywords: *Solanum nigrum*, endophytes, abiotic stress, bioactive metabolites, radical scavenging activity, ferric reducing power, antimicrobial activity

Posted Date: February 12th, 2025

DOI: <https://doi.org/10.21203/rs.3.rs-6002689/v1>

License: © ⓘ This work is licensed under a Creative Commons Attribution 4.0 International License. [Read Full License](#)

Additional Declarations: No competing interests reported.

Abstract

Bacterial endophytes isolated from medicinal and wild plant species have recently gained significant attention for their medicinal properties, often closely linked to those of their plant hosts. In this study, two endophytic *Bacillus* isolates were identified and taxonomically characterized using 16S rRNA sequencing and multi-locus sequence typing (MLST). We also investigated the impact of sublethal concentrations (0.5 mg/mL) of cadmium and hydrogen peroxide on metabolite production and bioactivity. Phytochemical testing, along with antimicrobial and antioxidant assays, revealed shifts in metabolite production under stress conditions. According to 16S rRNA-based similarity searches, both isolates share a close relationship with *Bacillus cereus* complex; however, phylogeny and MLST failed to resolve their species identity. Phytochemical screening of methanolic crude extracts from both isolates tested positive for alkaloids, flavonoids, and saponins. Notably, tannins were detected only after cadmium treatment, while steroids were present following exposure to both cadmium and H₂O₂. LC-MS fingerprinting confirmed the presence of several tannins and steroids in treated samples. The untreated crude extracts exhibited an IC₅₀ of ~ 3 mg/mL in the DPPH assay, which decreased to ~ 1.5 mg/mL after treatment with cadmium or H₂O₂, indicating a significant increase in radical scavenging activity. Additionally, extracts from both treated and untreated bacteria displayed antimicrobial activity against selected bacterial pathogens, with MIC values ranging from 62.5 µg/mL to 125 µg/mL. LC-MS analysis identified various antimicrobial and antioxidant metabolites, including phenoxymethylpenicilloyl, maculosin, (S,R,S)-alpha-tocopherol, 3-indoleacrylate, procyanidin A2, cis-11-eicosenamide, 3-hydroxy-3-phenacyloxindole, and 9-octadecenamide.

Introduction

Endophytic bacteria are key members of the plant endo-microbiome, colonizing plant tissues for variable periods without causing symptomatic infection. These microbes play a significant role in promoting plant health and productivity (Pandey et al., 2022). Notably, endophytic bacteria can produce secondary metabolites or natural products *in vitro* that mimic those generated *in vivo* by their host plants thereby, sharing similar medicinal properties (Tlou et al., 2024; Photolo et al., 2020). These metabolites exhibit a broad range of bioactivities, including anticancer, antioxidant (Photolo et al., 2020), immunomodulatory (Sharma et al., 2024), hepatoprotective (Kodoli et al., 2021), neuroprotective (Pant and Vasundhara, 2023), and antimicrobial effects (Tlou et al., 2024). As reservoirs of bioactive metabolites, these bacteria hold potential applications in diverse fields, including the food industry, agriculture, and pharmaceuticals, with profound implications for human health. Moreover, due to their symbiotic relationship with plants, endophyte-derived compounds are often less toxic to humans, making them especially appealing for therapeutic use (Narayanan and Glick, 2022). Bioprospecting of bacterial endophytes is regarded as a novel frontier in the search for valuable natural products, yielding over 7,360 bioactive metabolites to date (Demain, 2014; Abdel-Razek et al., 2020). This underscores the immense potential of endophytic bacteria in advancing drug development and promoting health and well-being.

In bacteria, secondary metabolites are encoded by biosynthetic gene clusters (BGCs), which consist of co-located genes that work together to synthesize complex molecules (Sharrar et al., 2020; Madema et al., 2015). These clusters typically contain genes encoding core "backbone" enzymes responsible for constructing the compound's primary structure, along with tailoring enzymes and, in some cases, regulatory proteins (Brakhage, 2013; Osbourn, 2010). Recent data indicate that approximately 11,000 BGCs have been identified across 9,000 bacterial genomes (Sharrar et al., 2020). However, a significant proportion of these BGCs remains uncharacterized, with no clear links to their corresponding metabolites. Furthermore, the factors influencing BGC activity are still largely unexplored (Rojas-Aedo et al., 2017). A key challenge in this field is the cryptic or silent expression of many BGCs, making their study in laboratory settings difficult.

This study explores the potential of abiotic stress to induce the production of novel secondary metabolites. In their natural environment, bacteria are frequently exposed to various stressors, prompting significant genetic and metabolic adaptations that can influence secondary metabolite production (Banothu and Uma, 2021; Baral et al., 2018). The relationship between stress-induced genetic responses and secondary metabolism is closely tied to the stationary phase of bacterial growth and global stress response mechanisms, as highlighted in studies by Tlou and Photolo (2020) and Baral et al. (2018). Understanding these processes may help unlock the potential of silent BGCs, thereby expanding the repertoire of bioactive compounds.

In vitro, the production of bioactive metabolites in bacteria is highly dependent on specific culturing conditions, which play a crucial role in regulating the metabolic pathways responsible for natural product synthesis and accumulation (Aftab, 2019). Stress factors, such as heavy metals, have been identified as effective in stimulating the synthesis of bioactive metabolites in endophytic bacteria (Dubey et al., 2019). According to Banothu and Uma (2021), exposure to high levels of heavy metals can generate reactive oxygen species (ROS), overwhelming bacterial antioxidant defences and triggering the production of antioxidant metabolites.

This study focuses on bacterial endophytes isolated from the medicinal plant *Solanum nigrum*, a dicot herbal species in the Solanaceae family, widely distributed across Europe, Asia, and Africa. While certain parts of *S. nigrum*, such as unripe fruits, contain toxic compounds like solanine and glycoalkaloids (Lee and Lim, 2006), other parts are used in traditional medicine for treating ailments such as stomach ulcers, ringworm, asthma, and fever (Hameed et al., 2017; Atanu et al., 2010). *S. nigrum* has also been documented to exhibit heavy metal tolerance through mechanisms such as enhanced antioxidant enzyme activity and the deposition of metals in non-active plant tissues (Rehman et al., 2017). This suggests that microorganisms associated with *S. nigrum* may also possess mechanisms for heavy metal tolerance.

To our knowledge, this is the first study to investigate the impact of stress on secondary metabolite production in bacterial endophytes isolated from *S. nigrum*. The research aims to identify and characterize these endophytic bacterial strains using phylogenetic and comparative techniques, including 16S rRNA gene sequencing and multilocus sequence typing (MLST). It also evaluates bacterial growth, metabolite production, and extraction processes. Additionally, advanced Liquid Chromatography-Quadrupole Time-of-Flight Tandem Mass Spectrometry (LC-MS/MS) is employed to identify bioactive metabolites.

Methods and Materials

Bacterial Strain and Maintenance

The two bacterial endophytes used in this study were generously provided by Prof. Serepa-Dlamini from the Department of Biotechnology, University of Johannesburg (South Africa). The bacterial cultures were preserved in 30% glycerol stock and routinely maintained on LB agar plates (composition per litre: peptone 10 g, sodium chloride 10 g, yeast extract 5 g, and agar 15 g; pH 7.0). The plates were incubated at 28°C for 24 hours to support culture maintenance.

For experimental growth, the bacteria were cultured in LB broth (composition per litre: peptone 10 g, sodium chloride 10 g, and yeast extract 5 g; pH 7.0) at 37°C with agitation at 120 rpm for 24 hours.

Genomic DNA extraction and polymerase chain reaction amplification and sequencing

Genomic DNA was extracted using the Zymo Quick-DNA™ Fungal/Bacterial Miniprep Kit following the manufacturer's instructions. The extracted DNA was analyzed on a 1% agarose gel via electrophoresis at 100 V and 200 mA. Visualization of DNA fragments was performed using a Bio-Rad gel documentation system (Lasec® Group, Cape Town, South Africa). DNA quantification was carried out using a NanoDrop™ ND-2000 UV-vis spectrophotometer (Thermo Fisher Scientific Inc., Waltham, USA).

The 16S rRNA gene for each bacterial endophyte was amplified according to the protocol by Tsuchida et al. (2002). Universal primers 27F (5'-AGAGTTTGATCTGGCTCAG-3') and 1492R (5'-AAGGAGGTGWTCCARCC-3') were used for 16S rRNA amplification, while seven housekeeping gene regions for *Bacillus cereus* were amplified for multilocus sequence typing (MLST), as detailed in Table 1. PCR reactions were conducted in 25 µL total volumes under the following conditions: an initial denaturation at 92°C for 2 minutes, followed by 30 cycles of denaturation at 92°C for 30 seconds, annealing at 52°C for 30 seconds, and extension at 72°C for 2 minutes. A final elongation step at 72°C for 2 minutes was performed, with termination at 4°C. The resulting amplicons were analysed on a 1% agarose gel under the same electrophoresis conditions and visualized using the Bio-Rad gel documentation system. Positive amplicons were excised from the gel, purified using the GeneJet Gel Extraction Kit, and sequenced via Sanger sequencing at Inqaba Biotechnical Industries (Pretoria, South Africa).

Table 1
MLST primer sequences
(<https://pubmlst.org/organisms/bacillus-cereus/primers>)

Name of Primer	Primer Sequence (5' to 3')
Bac-Gmk_F	ATTTAAGTGAGGAAGGGTAGG
Bac-Gmk_R	GCAATGTTACCAACCACAA
Bac-ivlD-F	CGGGGCAAACATTAAGAGAA
Bac-ivlD-R	GGTTCTGGTCGTTTCCATTC
Bac-Pta-F	GCAGAGCGTTTAGCAAAGAA
Bac-Pta-R	TGCAATGCGAGTTGCTTCT
Bac-Pur-F	CTGCTGCGAAAATCACAAA
Bac-Pur-R	CTCACGATTCGCTGCAATAA
Bac-PycA-F	GCGTTAGGTGGAACGAAAG
Bac-PycA-R	CGCGTCCAAGTTTATGGAAT
Bac-Tpi-F	GCCCAGTAGCACTTAGCGAC
Bac-Tpi-R	CCGAAACCGTCAAGAATGAT
Bac-Glp-F	GCGTTTGTGCTGGTGAAGT
Bac-Glp-R	CTGCAATCGGAAGGAAGAAG

Phylogenetic analysis

The CLC Bio Main Workbench was used to assemble forward and reverse sequencing reads, generating a consensus sequence for each bacterial isolate. A Basic Local Alignment Search Tool (BLAST) search was then performed on the National Center for Biotechnology Information (NCBI) GenBank nucleotide sequence database (<https://www.ncbi.nlm.nih.gov/genbank/>) to identify potential matches for each query sequence, as described by Altschul et al. (1997). Sequences closely matching the BLAST query results, along with their related taxa, were retrieved for phylogenetic analysis.

Multiple sequence alignment was performed using the Clustal X 2.1 tool (Thompson et al., 1994). Phylogenetic and molecular evolutionary analyses were conducted in MEGA X, utilizing the maximum likelihood method with 1,000 bootstrap replicates, as outlined by Kumar et al. (2018).

Bacterial growth, treatment, metabolite production and extraction

Bacterial growth

Bacterial growth analysis was performed following the method described by Tlou et al. (2024) with minor modifications. Briefly, a starter culture was prepared by inoculating a single bacterial colony into 5 mL of LB broth and incubating it overnight at 37°C with continuous shaking at 120 rpm. Subsequently, 0.5 mL of the starter culture was transferred into 50 mL of LB broth (composition per liter: tryptone 10 g, yeast extract 5 g, and sodium chloride 10 g; pH 7.0) and cultivated at 37°C with shaking at 120 rpm. Optical density (OD) measurements were taken in triplicate every 2 hours over a 48-hour period using the ONDA UV/VIS spectrophotometer (Lasec® Group, Cape Town, South Africa) at a wavelength of 600 nm.

Minimum inhibitory concentration for cadmium and hydrogen peroxide

For determining the MIC for the stressors, an overnight bacterial culture for each isolate was prepared in 10 mL of LB medium and incubated for 16–18 hours at 37°C. The cultures were then adjusted to a McFarland standard of 0.5 optical density. The minimum inhibitory concentration (MIC) was determined using the method described by Andrews (2001), with minor modifications. Positive controls consisted of tubes containing 2 mL of LB broth and 0.2 mL of overnight culture, while negative controls contained only LB broth. The experiments were performed in triplicate. MIC values were determined as the lowest concentration of Cd or H₂O₂.

Metabolite extraction

The extraction of crude secondary metabolites was carried out using the method previously described in (Balachandran et al., 2012) with minor modifications. Briefly, LB broth (1 L) was prepared in 2 L Erlenmeyer flasks and autoclaved at 121°C for 20 min. For the treated secondary metabolite each of the 2 L flasks was inoculated with the endophytic bacteria and incubated at 37°C for 8hrs, then sub lethal (0.5 mg/L) of H₂O₂ and cadmium was added to the flasks respectively and were further incubated for 7 days shaking at 120 rpm and then for the untreated samples each 2 L flasks of LB media was inoculated with the endophytic bacteria for 7 days. On 7th day, all the cultures were centrifuged at 10 000 rpm for 15 minutes for biomass removal. Equal volumes of ethyl acetate and chloroform (1 :1 v/v) were added to the supernatant followed by vigorous shaking. The organic solvent layer was collected in a boiling flask, and it was further concentrated using a vacuum rotary evaporator (Lasec® Group, Cape town, South Africa) at 40°C. The crude extracts were transferred to a 5mL sterile vials and left to dry at room temperature. The phytochemical screening of crude extract was adopted from Harbourne (1983) and Trease and Evans (1983) with minor modifications shown in Table 3.

Antioxidant assay

Scavenging 2, 2-Diphenyl-1-picrylhydrazyl (DPPH) Free Radical Assay

The antioxidant activity of the endophytic bacterial isolates was evaluated using the 2,2-diphenyl-1-picrylhydrazyl (DPPH) free radical scavenging assay, following the method described by Takao et al. (2015) with minor modifications. Briefly, extracts of the endophytic bacterial isolates and ascorbic acid (used as a positive control) were dissolved in methanol to achieve an initial concentration of 12.5 mg/mL. These were then mixed with 200 µM methanolic DPPH solution to prepare final concentrations of 12.5, 6.25, 3.125, 0.781, 0.195, 0.097, and 0.048 mg/mL in a 96-well plate (Greiner Bio-One GmbH, Germany). Methanol served as the solvent control.

The plates were incubated at 25°C for 30 minutes, and absorbance was measured at 517 nm using a microplate reader (Multiskan GO, Thermo Fisher Scientific Inc., Waltham, USA). All experiments were performed in triplicate, and the IC₅₀ was determined graphically. The percentage inhibition was calculated using the formula:

$$\% \text{Inhibition} = \frac{(\text{absorbance of control} - \text{absorbance of the sample})}{\text{absorbance of control}} \times 100$$

Ferric Reducing Antioxidant Power assay

The ferric reducing antioxidant power (FRAP) assay was performed using a SIGMA-ALDRICH kit (Sigma-Aldrich, Darmstadt, Germany) according to the manufacturer's instructions. The assay measures the reducing potential of an antioxidant, which reacts with a ferric tripyridyl triazine (Fe^{3+} -TPTZ) complex to produce a blue-colored ferrous tripyridyl triazine (Fe^{2+} -TPTZ) complex, resulting in an increased absorbance at 593 nm (Adebiyi et al., 2017).

Reagents were prepared as follows: the endophytic bacterial isolate extract was dissolved in methanol to achieve an initial concentration of 12.5 mg/mL. The positive control was prepared by mixing 4 μL of the control substance with 6 μL of FRAP assay buffer to make a total volume of 10 μL . A 190 μL reaction mix was prepared by combining 152 μL of FRAP assay buffer, 19 μL of FRAP probe, and 19 μL of FeCl_3 solution. A standard curve was generated using a 2 mM ferrous standard with varying dilutions, as outlined in Table 2.

For the assay, 20 μL of the endophytic bacterial extract was added to the first well, followed by two-fold serial dilutions to achieve final concentrations of 12.5 mg/mL, 6.25 mg/mL, 3.125 mg/mL, 0.781 mg/mL, 0.195 mg/mL, 0.097 mg/mL, and 0.048 mg/mL. Each well, including the endophytic bacterial isolate extract wells, standard wells, and positive control wells, received 190 μL of the reaction mix. The plate was incubated for 60 minutes at 37°C, and absorbance was immediately measured at 594 nm.

Antimicrobial assay

The Minimum Inhibitory Concentration (MIC) of the crude extracts from the isolates was determined using the methodology described by Andrews (2001), with slight modifications. Briefly, stock solutions were prepared by dissolving 1 mg of each extract in 1 mL of 1 M DMSO, yielding a final concentration of 1 mg/mL. Serial dilutions of the stock solutions were then prepared using tryptic soy broth (g/L: casein peptone (pancreatic) 17, dipotassium hydrogen phosphate 2.5, glucose 2.5, sodium chloride 5, and soy peptone 3) to achieve final concentrations of 500, 250, 125, 62.5, 31.25, 15.625, 7.813, 3.906, and 1.953 $\mu\text{g/mL}$.

The pathogenic test strains included *Salmonella enterica* DSS_NWU (GenBank Accession Number: CP123007), *Escherichia coli* (ATCC 25922), *Staphylococcus aureus* (ATCC 26923), and *Enterococcus durans* NWUTAL1 (GenBank Accession Number: VMRQ00000000) (Foka et al., 2020). These strains were standardized to the McFarland 0.5 standard, and 50 μL of each pathogen culture was inoculated into 15 mL of tryptic soy broth, followed by incubation at 37°C for 24 hours. For the MIC assay, 100 μL of each pathogenic strain was added to the wells of a 96-well microtiter plate horizontally, while 100 μL of the crude extract dilutions were added vertically, beginning with the highest concentration. Positive controls, including ampicillin and streptomycin, and a negative control (DMSO) were also included. The plate was sealed with parafilm and incubated at 37°C for 16–20 hours. After incubation, 10 μL of iodinitrotetrazolium chloride solution (4 mg/mL) was added to each well. The MIC was defined as the lowest concentration of the extract that resulted in a clear well, indicating the inhibition of microbial growth. All antimicrobial experiments were conducted in triplicate ($n = 3$) to ensure reproducibility.

Liquid Chromatography-Quadruple Time-of-Flight Tandem Mass Spectrometry (LC-MS/MS)

Extracts were analyzed using a Shimadzu LCMS-9030 qTOF instrument (Shimadzu Corporation, Kyoto, Japan). Chromatographic separation was performed on a Shim-pack Velox C18 column (100 mm \times 2.1 mm, 2.7 μm particle size) at 55°C. A 3 μL injection volume was used for all samples, and separation was achieved with a binary mobile phase gradient: solvent A (0.1% formic acid in Milli-Q water, HPLC grade) and solvent B (methanol with 0.1% formic acid, UHPLC grade). The flow rate was maintained at 0.3 mL/min over a 20-minute gradient: 5% B for 3 minutes, 5–40% B (3–5 min), 40–95% B (5–12 min), 95% B held (12–16 min), then returned to 5% B (16–18 min), maintained for 2 minutes, followed by a 3-minute column re-equilibration.

The chromatographic effluent was analyzed using a qTOF high-definition mass spectrometer in negative electrospray ionization mode. Instrument parameters were set as follows: interface voltage 4.0 kV, interface temperature 300°C, nebulization/dry gas flow 3 L/min, heat block temperature 400°C, DL temperature 280°C, detector voltage 1.8 kV, and flight tube temperature 42°C. Sodium iodide (NaI) was used for high-mass accuracy calibration. MS1 and MS2 data (via data-dependent acquisition) were collected for ions with m/z 100–1000 exceeding an intensity threshold of 5000. Fragmentation experiments used argon as the collision gas, with a collision energy of 30 eV (\pm 5 eV spread).

Quality control (QC) pooled samples were injected at the start and end of the batch to ensure system equilibration and non-linear signal correction. Additionally, sample acquisition was randomized, with QC samples analyzed every 10 injections to monitor instrument response stability.

Metabolite identification was performed using SIRIUS software (version 4.9.12) as described by Dührkop et al. (2019). Raw LC-MS data were converted to mzML format before import into SIRIUS. Molecular formula computation was conducted with qTOF as the instrument type, mass accuracy set at 10 ppm, and $[\text{M}-\text{H}]^+$ as the ionization mode. Element searches focused on C, H, N, and O, with a maximum of 10 candidates. Structure elucidation via CSI: FingerID used comprehensive database searches with $[\text{M}-\text{H}]^+$ as the sole adduct, following Dührkop et al. (2015). Additionally, Canopus Class Prediction was enabled, based on the methodology of Hoffmann et al. (2021).

Results

Molecular identification

To molecularly identify the bacterial isolates, the 16S rRNA gene was sequenced using universal primers 27F and 1492R. Sequencing data revealed that *Bacillus* sp. NV1 and 35 shared $\geq 99\%$ identity with reference strains *Bacillus cereus* and *Bacillus anthracis*, respectively (Table 2A). The obtained 16S rRNA sequences were submitted to the National Center for Biotechnology Information (NCBI) and assigned accession numbers, as listed in Table 2A.

The *Bacillus cereus* MLST scheme was chosen to determine the identities of the isolates *Bacillus* sp. NV1 and 35. Table 2B presents the allelic profiles obtained from MLST, revealing that both Sample 1 and Sample 35 share identical allelic profiles across all housekeeping gene loci. This indicates that there are no genetic differences between these strains, suggesting they belong to the same sequence type. However, since no specific sequence types are assigned for *Bacillus cereus*, these profiles may not correspond to *Bacillus cereus* itself but rather to an uncharacterized strain within the database.

Table 2

A. NCBI Blast results for the 16S rRNA sequencing from *Bacillus* sp. NV1 and 35 bacterial endophytes.

Strains/isolates	Assigned bacterial name	Assigned GenBank accession number	NCBI BLAST Results			
			Closely related species with accession number	E-value	Query cover %	Percentage identity
<i>Bacillus</i> sp. NV1	<i>Bacillus</i> sp. strain NV1	OQ929927.1	<i>Bacillus cereus</i> strain AFS014582 OP986968.1	0	99%	99.37%
<i>Bacillus</i> sp. NV35	<i>Bacillus</i> sp. strain NV 35	OQ931240	<i>Bacillus anthracis</i> strain Ohio ACB OP009341.1	0	100%	99.35%

Table 2

B: Allelic profiles and sequence types obtained for *Bacillus* sp. 1 and 35

Sample Name	Gmk	lvd	Pta	Pur	PycA	Tpi	Glp	ST
NV1	39	553	53	468	80	94	197	-
NV35	39	553	53	468	80	94	197	-

Phylogenetic analysis of the 16S rRNA sequences of the isolates, along with sequences retrieved from NCBI, was conducted using MEGA X with the maximum likelihood method and 1,000 bootstrap replicates. The results showed that both endophytic bacterial isolates clustered with closely related *Bacillus* species. In the phylogenetic tree, *Bacillus* sp. strain NV 1 formed a monophyletic relationship with *Bacillus cereus*, while *Bacillus* sp. strain NV 35 exhibited a distinct phylogenetic placement among other *Bacillus* species, including *Bacillus* sp. strain NV 1 (Fig. 1).

Bacterial growth, treatment, and metabolite extraction

The bacterial isolates were cultured in LB broth for 72 hours to monitor their growth dynamics. Both *Bacillus* isolates exhibited similar growth patterns, reaching the stationary phase within 8 hours of inoculation (data not shown). The stationary phase was selected for stress induction and secondary metabolite extraction, as it is commonly associated with the production of bioactive compounds in fermentation media following microbial growth completion.

To determine the sub-lethal concentration of cadmium and hydrogen peroxide, the broth dilution method was used. The results indicated that the minimum inhibitory concentration (MIC) for both cadmium and hydrogen peroxide was 0.5 mg/mL (data not shown).

Phytochemical testing

Several phytochemical tests were conducted to screen for alkaloids, flavonoids, steroids, tannins, and saponins. The results revealed that both treated and untreated *Bacillus* sp. strains NV1 and 35 exhibited the presence of alkaloids, flavonoids, and saponins (Table 3). Additionally, extracts from *Bacillus* sp. strains NV1 and 35, when treated with H₂O₂ and cadmium, respectively, tested positive for steroids and showed the presence of tannins (Table 3).

Table 3

Phytochemical analysis of methanolic crude extracts from bacteria endophytes. The (+) and (-) represent the presence and absence of the phytochemicals.

Phytochemical Test	Procedure	Observation	<i>Bacillus</i> sp. NV1			<i>Bacillus</i> sp. NV35		
			Untreated	Cadmium	H ₂ O ₂	Untreated	Cadmium	H ₂ O ₂
Alkaloids	In 1ml of endophyte extract add 2-3 drops of Dragendorff's reagent.	Precipitation or turbidity formation (+)	+	+	+	+	+	+
Flavonoids	In 1ml of endophyte crude extract add 2-3drops of (NaOH).	Yellow colour (+)	+	+	+	+	+	+
Saponins	In 5ml of the crude extract and 3 drops of olive oil	Formation of foam (+)	+	+	+	+	+	+
Steroids	In 1ml of the crude extract add 1ml of CHCl ₃ , and 3 drops of conc.H ₂ SO ₄	Reddish brown ring (+)	-	+	+	-	+	+
Tannins	In 1ml of the crude extract add 3 drops of FeCl ₃	Blackish blue or Blackish-green colour (+)	-	+	-	-	+	-

Antioxidants Assay

The DPPH free radical scavenging assay was used to evaluate the antioxidant activity of the crude extracts. For each bacterial isolate, results were analyzed using separate graphs comparing the untreated extract with the two treated extracts. The assay confirmed that all bacterial isolates exhibited free radical scavenging activity across all tested concentrations (0.048–12.5 mg/mL), with inhibition percentages ranging from 27–80% (Fig. 2A & 2B). Among the isolates, cadmium-treated extracts demonstrated the highest radical scavenging activity, followed by H₂O₂-treated extracts (Fig. 2A & 2B).

Figure 2.A: Fig. 2B. DPPH free radical scavenging activity of *Bacillus* sp. NV1 methanolic crude extracts (n = 3), p values less than 0.05 were statistically different. Vitamin C was used as a positive control.

The endophytic extracts exhibited higher IC₅₀ values, ranging from 1.353 to 3.339 mg/mL, compared to vitamin C, which had an IC₅₀ value of 3.99 µg/mL. This indicates that vitamin C had a lower antioxidant potential than the endophytic extracts. Among the crude extracts, those from *Bacillus* sp. strains NV1 and 35 treated with cadmium demonstrated the highest antioxidant activity, as they had the lowest IC₅₀ values of 2.453 and 1.353 µg/mL, respectively (Table 4).

Table 4
IC₅₀ values of methanolic crude extracts from *Bacillus* sp. NV1 and 35 using Microsoft EXCEL.

	Ascorbic acid	<i>Bacillus</i> sp. NV1			<i>Bacillus</i> sp. NV35		
		Untreated	Cadmium	H ₂ O ₂	Untreated	Cadmium	H ₂ O ₂
IC50 Values (mg/mL)	3,99	3,339	2.453	2.97	3.233	1.353	2.46

Ferric reducing antioxidant activity (FRAP) assay

To further confirm the antioxidant activity of the crude extracts, the Ferric Reducing Antioxidant Power (FRAP) assay was performed. The ferric reducing power of the positive standard was significantly higher than that of the extracts from *Bacillus* sp. NV1. Across all tested concentrations, the cadmium-treated crude extracts exhibited the highest ferrous equivalent concentrations in *Bacillus* sp. NV1, while the untreated extract showed the lowest ferric-reducing activity (Fig. 3A). In *Bacillus* sp. NV35, the cadmium-treated crude extracts demonstrated ferric-reducing activity comparable to the positive control at various concentrations, indicating strong antioxidant potential (Fig. 3B).

Antimicrobial Assay

The extracts from all isolates were tested for antibacterial activity against four pathogenic strains: Gram-negative bacteria *Escherichia coli* and *Salmonella* sp., and Gram-positive bacteria *Staphylococcus aureus* and *Enterococcus durans*. The minimum inhibitory concentration (MIC) of the crude extracts for all isolates ranged from 62.5 µg/mL to 125 µg/mL. Notably, the methanolic crude extract of *Bacillus* sp. strain 35NV35, treated

with both cadmium and hydrogen peroxide, exhibited lower MIC values (62.5 µg/mL) against *Salmonella* sp. compared to the positive control (ampicillin) (Table 5).

Table 5
MIC values of antimicrobial activities for endophytic bacterial extracts.

Bacterial strain	<i>Bacillus</i> sp. NV35 (µg/ml)			<i>Bacillus</i> sp. NV35 (µg/ml)			Ampicillin (µg/ml)
	Untreated	Cd	H ₂ O ₂	Untreated	Cd	H ₂ O ₂	
<i>Staphylococcus aureus</i> (ATCC26923)	125	125	125	125	125	125	62.5
<i>Enterococcus durans</i> (NWUTAL1)	125	125	125	125	125	125	15.625
<i>Salmonella enterica</i> (DSS_NWU)	125	125	125	125	62.5	62.5	125
<i>Escherichia coli</i> (ATCC25922)	125	125	125	125	125	62.5	15.625

Liquid Chromatography-Quadruple Time-of-Flight Tandem Mass Spectrometry

The LC-qTOFMS was used to identify the compounds responsible for the antimicrobial and antioxidant activities in bacterial endophyte extracts. Identification was based on retention times (RT), parent masses, and molecular formulas, as detailed in Table 6. The analysis revealed a diverse range of bioactive compounds, including fatty acids, alkaloids, flavonoids, peptides, tannins, steroids, and phenolic compounds. Additionally, stress-induced metabolites were detected. These chemical classes are well known for their antimicrobial and antioxidant properties, aligning with the observed bioactivity of the extracts.

Table 6

Bioactive metabolites identified from the crude extracts for the bacterial isolates. Nt = untreated, Cd = cadmium, H₂O₂ = hydrogen peroxide.

Parent mass	RT mean	Compounds	Chemical formula	Bacillus sp. strain1			Bacillus sp. NV35			Bioactivity/ Applications
				Nt	Cd	H ₂ O ₂	Nt	Cd	H ₂ O ₂	
575.32	14.88	H-Leu-Pro-Val-Pro-Gln-OH	C ₂₆ H ₄₄ N ₆ O ₇	✓	✓	✓	✓	✓	✓	Antihypertensive, Antibacterial, food additives, cosmetic, antioxidative, anti-inflammatory (Zaky <i>et al.</i> , 2022)
504.39	15.12	N-hexadecyloctadeca-9,12-dienamide	C ₃₄ H ₆₅ NO	✓	✓	✓	✓	✓	✓	Neuroprotection, anti-microbial, antioxidant (Battista <i>et al.</i> , 2019)
409.33	15.736	Beta-hexaprene	C ₃₀ H ₄₈	✓	✓	✓	✓	✓	✓	No activity reported
507.45	17.18	N,N'-bis(2,2,6,6-tetraethylpiperidin-4-yl)hexane-1,6-diamine	C ₃₂ H ₆₆ N ₄	✓	✓	✓	✓	✓	✓	antitumor activity, anti-cancer, antiviral, analgesic properties, cardiovascular disease (Abd Rani <i>et al.</i> , 2022)
205.116	4.87	Diethyl 1-(2-(1,3-dioxoisindolin-2-yl)butanoyl)-2,6-dimethyl-4-(3-nitrophenyl)-1,4-dihydropyridine-3,5-dicarboxylate	C ₃₁ H ₃₁ N ₃ O ₉	✓	✓	✓	✓	✓	✓	Antimicrobial activity (Al-Majedy <i>et al.</i> , 2017)
366.373	15.23	(S,R,S)-alpha-Tocopherol	C ₂₉ H ₅₀ O ₂	✓	✓	✓	✓	✓	✓	Anti-aging, anti-diabetic, antioxidant, anti-inflammatory, anticancer (Hameed <i>et al.</i> , 2015)
366.18	3.29	1-(2,3,4,6-tetra-O-acetyl-d-glucopyranosyl)-5-nitro-1h-1,2,4-triazole	C ₁₆ H ₂₀ N ₄ O ₁₁	✓	✓	✓	✓	✓	✓	antimicrobial, anticonvulsant, antidepressant, antihypertensive (Satharwa,, 2016)
254.2	12.27	Palmitoleamide	C ₁₆ H ₃₁ NO					✓		Antibacterial (Zaher <i>et al.</i> , 2014)
502.498	14.31	3-(4'-Methoxyphenyl)-5-phenyl-2, 4-pentadiene-1-one	C ₃₄ H ₆₃ NO	✓	✓			✓		antimicrobial activity, antifungal activity (Sharma and Sharma, 2010)
366.35	15.34	(1R,2R,5R,8R,9R,10R,13R,14S,18R)-1,2,5,14-tetramethyl-17-propan-2-ylidene-8-prop-1-en-2-ylpentacyclo [11.7.0.0.02,10.05,9.014,18] icosane	C ₃₀ H ₄₈		✓	✓		✓	✓	Anti-aging, analgesic, anti-diabetic, antioxidant, anti-inflammatory (Shaikh <i>et al.</i> , 2012)

Parent mass	RT mean	Compounds	Chemical formula	Bacillus sp. strain1			Bacillus sp. NV35			Bioactivity/ Applications
				Nt	Cd	H ₂ O ₂	Nt	Cd	H ₂ O ₂	
573.48	15.95	Fahfa 24:4/13:0	C ₃₇ H ₆₄ O ₄				✓			Anti-iabetes, anti-inflammatory (Tan et al.,2019)
594.9	11.49	Tris (3-methoxy-4-hydroxybenzoic acid)1,2,4-benzenetriyl ester	C ₃₀ H ₂₄ O ₁₂		✓			✓		Antibacterial, antifungal, hepatoprotective (Zhongze et al, 2008)
603.53	14.82	2-(N-((2'-(2H-tetrazole-5-yl)-[1,1'-biphenyl]-4yl)-methyl)-pentanamido)-3-methyl butanoic acid	C ₃₂ H ₆₇ NO ₆	✓			✓			Antihypertensive, Antioxidant (Masood et al.,2023)
361.17	1.29	2-Methyl-1-(4-propan-2-ylphenyl) pentan-3-one	C ₁₅ H ₂₂ O		✓		✓	✓		No activity reported
261.12	5.76	Maculosin	C ₁₄ H ₁₆ N ₂ O ₃	✓	✓	✓	✓	✓	✓	Antioxidant, anti-cancer and non-toxicity (Pawle and Singh, 2014) et al., 2021)
369.11	2.56	Phenoxomethylpenicilloyl (penicilloyl V)	C ₁₆ H ₂₀ N ₂ O ₆ S	✓				✓	✓	Antimicrobial activity (Stuart et al., 2009)
310.31	13.59	cis-11-Eicosenamide	C ₂₀ H ₃₉ NO		✓		✓	✓	✓	Antimicrobial activity, Biocontrol (Qi et al., 2022)
577.13	11.50	Procyanidin A2	C ₃₀ H ₂₄ O ₁₂	✓	✓	✓	✓	✓	✓	Antioxidant, antimicrobial, and anti-inflammatory (Wang et al., 2020)
250.09	12.50	Cinchophen	C ₁₆ H ₁₁ NO ₂	✓	✓	✓	✓	✓	✓	Antimicrobial (Ezalarab et al., 2023)
284.29	13.45	Octadecanamide	C ₁₈ H ₃₇ NO			✓			✓	Antimicrobial (dos Reis et al., 2019)
602.52	13.37	N,N'-{[(Undec-10-enoyl)azanediyl]di(ethane-2,1-diy)}di(undec-10-enamide)	C ₃₇ H ₆₇ N ₃ O ₃			✓			✓	No activity reported
188.07	4.95	3-Indoleacrylate	C ₁₁ H ₉ NO ₂	✓			✓			Antioxidants, anti-inflammatory properties (Wlodarska et al., 2017)

Discussion and conclusions

The identification and characterization of bacterial isolates is often achieved using a combination of molecular techniques, including 16S rRNA sequencing, phylogenetic analysis, and Multi-Locus Sequence Typing (MLST). The 16S rRNA gene, a widely accepted molecular marker, is invaluable for bacterial identification due to its conserved presence across prokaryotes and its 1500-base pair length, which provides sufficient sequence data for species-level classification. Additionally, the 16S rRNA gene's reduced susceptibility to horizontal gene transfer and its variable regions, which help distinguish different taxonomic groups, make it a robust tool for bacterial identification (Clarridge, 2004; Kitahara and Miyazaki, 2013).

In our study, the 16S rRNA-based phylogenetic tree shows the evolutionary relationships between different *Bacillus* species, along with an *Escherichia coli* strain included in the analysis. The two isolates (*Bacillus sp.* NV35 and *Bacillus sp.* NV1) cluster together, suggesting they are closely related. Furthermore, the isolates (NV35 and NV1) are in a clade that is distinct from *Bacillus cereus* (OP986968.1 *Bacillus cereus* strain AFS014582). Instead, they are more closely related to *Bacillus sp. strain L18* (MT516451.1), rather than to the *Bacillus cereus* reference strain. The tree has multiple bootstrap values of 86, indicating relatively strong support for the clustering of these taxa. The node linking NV35 and NV1 to *Bacillus sp. strain L18* has a bootstrap value of 100, suggesting very high confidence in this relationship (Russo and Selvatti, 2018).

Since the isolates (NV35 and NV1) do not group directly with *Bacillus cereus*, this suggests they may belong to a different species or an uncharacterized strain within the *Bacillus* genus (Alnajar and Gupta, 2017). Therefore, the classification as *Bacillus sp.* rather than *Bacillus cereus* aligns with the MLST results (See Table 2B), where the specific sequence type could not be assigned to *B. cereus*. These findings underscore the need for more advanced methods, such as whole-genome sequencing, to resolve species-level identities with greater precision, as demonstrated by Diale et al. (2021). Such comprehensive genomic approaches will provide a more accurate and complete characterization of bacterial isolates, improving our understanding of their phylogenetic relationships and functional potential.

In this study, both isolates reached the stationary growth phase around 8 hours post-inoculation, and this phase was selected for the extraction of secondary metabolites. The stationary phase is a critical period in bacterial growth, during which cells typically begin to produce secondary metabolites. This occurs as the bacteria face various physical and chemical stresses, such as nutrient depletion and oxidative stress, which are characteristic of this phase (Ruiz et al., 2010; Jaishankar and Srivastava, 2017). Interestingly, both *Bacillus* isolates exhibited a similar growth profile when cultured in LB broth, suggesting a genus-specific growth pattern. This consistent behaviour highlights the close relationship between the two isolates and pointed to the potential similarities in their metabolic responses to the stress conditions.

The phytochemical screening of crude extracts from *Bacillus sp.* NV1 and 35 revealed the presence of alkaloids, flavonoids, saponins but only tested positive for tannins, and steroids (Table 3) when exposed to the stressors. These findings suggest that the bacteria share some common biosynthetic pathways for secondary metabolites with their host plant, *Solanum nigrum*, which is known to be rich in bioactive compounds such as steroidal saponins, alkaloids, phenols, glycoalkaloids, glycoproteins, and polysaccharides (Liu et al., 2022). The production of bioactive compounds by endophytes is thought to be linked to the evolutionary relationship between the host plant and its microorganisms, which may have acquired genetic information from plants via horizontal gene transfer (Tiwari and Bae, 2020; Taghavi et al., 2005). Additionally, the presence of tannins and steroids in the treated crude extracts may result from the activation of previously silenced biosynthetic gene clusters (BGCs) that produce secondary metabolites in response to stressors, cadmium and H₂O₂, as suggested by previous studies (Wang et al., 2014; Jiang et al., 2014). Metals such as Fe, Cu, Mn, Zn, Co, Ni, Mo, Cd, and Mg and play vital roles in many microbial enzyme functions involved which includes secondary metabolite biosynthesis (Dubey et al., 2019).

The antimicrobial activity of the crude extracts was evaluated against four pathogenic strains: *Escherichia coli*, *Salmonella enterica*, *Staphylococcus aureus*, and *Enterococcus durans*. The results demonstrated that the extracts were effective against all test strains, with minimum inhibitory concentrations (MICs) ranging from 62.5 to 125 µg/mL. According to Van Vuuren (2008), extracts with an MIC of 1000 µg/mL or lower are considered significantly active, indicating strong antimicrobial potential in this study. Notably, extracts from *Bacillus sp.* NV35 treated with hydrogen peroxide and cadmium exhibited superior antimicrobial activity (6.25 µg/mL) against *S. enterica* compared to 125 µg/mL recorded for both the positive control and untreated extracts. This suggests that abiotic stress conditions may enhance or activate the production of antimicrobial bioactive compounds. These findings highlight the potential of endophytic bacteria as valuable sources of bioactive antimicrobial compounds (Table 5). Additionally, the results align with previous studies reporting antimicrobial compound production by *Bacillus* endophytes (Numan et al., 2022; Mohamad et al., 2018). Furthermore, the presence of alkaloids, flavonoids, and phenolic compounds in this study supports their well-documented antimicrobial and antioxidant properties (Ademović et al., 2017; Rehman & Khan, 2017; Martins et al., 2016; Yin et al., 2016).

The antioxidant activity of the crude extracts was evaluated using the DPPH free radical scavenging assay, a widely used method for assessing radical scavenging activity in natural products (Narkhede & Jagtap, 2015). To further validate the results, the more sensitive ferric reducing antioxidant power (FRAP) assay was also performed (Baliyan et al., 2022), with ascorbic acid serving as the standard control. Extracts from *Bacillus sp.* NV1 and NV35 demonstrated significant antioxidant properties, exhibiting IC₅₀ values lower than that of ascorbic acid, indicating superior radical scavenging activity (Molyneux, 2004).

The FRAP assay further supported these findings, revealing that extracts treated with hydrogen peroxide and cadmium exhibited higher antioxidant activity than untreated samples. This may be attributed to oxidative stress induced by hydrogen peroxide and metal ions, which has been reported to stimulate bacteria to produce antioxidant metabolites, phytohormones, and enzymes as a defence mechanism (Bilal et al., 2018; Seixas et al., 2022). The strong antioxidant activity observed in the endophytic crude extracts is likely due to the presence of phenolic compounds, flavonoids, tannins, and terpenoids—bioactive compounds previously reported for their potent antioxidant properties (Rahwati et al., 2019; Zaets & Kozyrovska, 2014). These compounds were identified in the crude extracts through phytochemical analysis and LC-MS detection.

This study identified several bioactive compounds, including H-Leu-Pro-Val-Pro-Gln-OH, N-hexadecyloctadeca-9,12-dienamide, octadecanamide, cinchophen, palmitoleamide, cis-11-eicosenamide, and phenoxomethylpenicilloyl, all of which have been previously reported for their antimicrobial

properties. Notably, all isolates produced fatty acid amide derivatives, which are generally associated with enhanced antimicrobial activity compared to their unmodified counterparts (Khare et al., 2009). These compounds are also commonly found in medicinal plants, reinforcing the idea that endophytes can synthesize bioactive compounds similar to those of their host plants. This indicates that endophytes could serve as alternative sources of valuable bioactive metabolites. Additionally, the compound palmitoleamide, detected in a *Bacillus* sp. NV35 extract treated with cadmium, is known for its antimicrobial properties (Zaher et al., 2015), which may explain the strong antibacterial effects observed in this extract. This finding also highlights how abiotic stress can influence secondary metabolite production, thereby enhancing the bioactivity of the extracts.

The study further demonstrated significant antioxidant activity, likely attributed to the presence of flavonoids, alkaloids, and phenolic compounds in the crude extracts, as confirmed by phytochemical testing and LC-MS analysis (Table 6). Phenolic compounds and flavonoids possess an ideal chemical structure for free radical scavenging activity (Kannan et al., 2016). Specific compounds such as (S,R,S)-alpha-tocopherol, 3-indoleacrylate, procyanidin A2, and maculosin are well-documented for their antioxidant properties both in vitro and in vivo (Ademović et al., 2017; Rehman & Khan, 2017; Martins et al., 2016; Yin et al., 2016). For example, alpha-tocopherol acetate (vitamin E acetate) is widely recognized for its ability to neutralize free radicals (Jiang, 2014), while Wang et al. (2020) highlighted the antioxidant potential of procyanidin A2.

Flavonoids, alkaloids, and phenolic compounds act as both primary and secondary antioxidants, playing a crucial role in reducing lipid peroxidation and providing effective antioxidant protection (Kaur et al., 2020). Moreover, the presence of tannins and steroids—including compounds such as N,N'-[[[(Undec-10-enoyl)azanediyl]di(ethane-2,1-diyl)]di(undec-10-enamide), Tris(3-methoxy-4-hydroxybenzoic acid)1,2,4-benzenetriyl ester, and (1R,2R,5R,8R,9R,10R,13R,14S,18R)-1,2,5,14-tetramethyl-17-propan-2-ylidene-8-prop-1-en-2-ylpentacyclo[11.7.0.0.2,10.05,9.014,18]icosane—suggests that abiotic stress may have triggered the activation of biosynthetic gene clusters, leading to the production of these bioactive metabolites.

Declarations

Author Contribution

M.G.T: Writing – review & editing, Writing – original draft, Supervision, Resources, Project administration, Methodology, Funding acquisition, Formal analysis, Data curation, Conceptualization. B.N: Writing – review & editing, Software, Methodology, Investigation, Data curation. N.M.M: Writing – review & editing, Software, Methodology, Investigation. B.B: Writing, methodology and investigation.

Acknowledgement

The authors would like to thank the Professor Mahloro Serepa-Dlamini (Department of Biotechnology, University of Johannesburg) for donating the bacterial isolates used in this study.

Data Availability

The datasets presented in this study can be found in online repositories. The names of the repository/repository and accession number(s) can be found at: <https://www.ncbi.nlm.nih.gov/genbank/OQ929927.1>; OQ931240

References

1. Abd Rani, N.Z., Lee, Y.K., Ahmad, S., Meesala, R. and Abdullah, I., 2022. Fused tricyclic guanidine alkaloids: Insights into their structure, synthesis and bioactivity. *Marine Drugs*, 20(9), p.579.
2. Ademović, Z., Hodžić, S., Halilić-Zahirović, Z., Husejnagić, D., Džananović, J., Šarić-Kundalić, B. and Suljagić, J., 2017. Phenolic compounds, antioxidant and antimicrobial properties of the wild cherry (*Prunus avium* L.) stem. *Acta Periodica Technologica*, (48), pp.1-13.
3. Aftab, T., 2019. A review of medicinal and aromatic plants and their secondary metabolites status under abiotic stress. *Journal of Medicinal Plants*, 7(3), pp.99-106.
4. Al-Majedy, Y. K., Kadhum, A. A. H., Al-Amiery, A. A., & Mohamad, A. B. (2017). Coumarins: The Antimicrobial agents. *Systematic Reviews in Pharmacy*, 8(1). Alnajar, S., & Gupta, R. S. (2017). Phylogenomics and comparative genomic studies delineate six main clades within the family Enterobacteriaceae and support the reclassification of several polyphyletic members of the family. *Infection, Genetics and Evolution*, 54, 108-127.
5. Altschul, S.F., Madden, T.L., Schäffer, A.A., Zhang, J., Zhang, Z., Miller, W. and Lipman, D.J., 1997. Gapped BLAST and PSI-BLAST: a new generation of protein database search programs. *Nucleic acids research*, 25(17), pp.3389-3402.
6. Andrews, J. M. 2001. Determination of minimum inhibitory concentrations. *Journal of antimicrobial Chemotherapy*, 48, pp.5-16.

7. Atanu, F.O., Ebiloma, U.G. and Ajayi, E.I., 2011. A review of the pharmacological aspects of *Solanum nigrum* Linn. *Biotechnol Mol Biol Rev*, 6(1), pp.1-7.
8. Balachandran, C., Duraipandiyan, V. and Ignacimuthu, S., 2012. Cytotoxic (A549) and antimicrobial effects of *Methylobacterium* sp. isolate (ERI-135) from Nilgiris forest soil, India. *Asian Pacific Journal of Tropical Biomedicine*, 2(9), pp.712-716.
9. Baliyan, S., Mukherjee, R., Priyadarshini, A., Vibhuti, A., Gupta, A., Pandey, R.P. and Chang, C.M., 2022. Determination of antioxidants by DPPH radical scavenging activity and quantitative phytochemical analysis of *Ficus religiosa*. *Molecules*, 27(4), p.1326.
10. Banothu, V. and Uma, A., 2022. Effect of biotic and abiotic stresses on plant metabolic pathways. *Phenolic Compounds—Chemistry, Synthesis, Diversity, Non-Conventional Industrial, Pharmaceutical and Therapeutic Applications*.
11. Baral, B., Akhgari, A. and Metsä-Ketelä, M., 2018. Activation of microbial secondary metabolic pathways: Avenues and challenges. *Synthetic and Systems Biotechnology*, 3(3), pp.163-178.
12. Brakhage A. A. (2013). Regulation of fungal secondary metabolism. *Nat. Rev. Microbiol.*, 11, 21–32.
13. Battista, N., Bari, M. and Bisogno, T., 2019. N-acyl amino acids: metabolism, molecular
14. Bharose, A.A. and Gajera, H.P., 2018. Antifungal activity and metabolites study of *Bacillus* strain against aflatoxin producing *Aspergillus*. *Journal of Applied Microbiology and Biochemistry*, 2(2), pp.1-8.
15. Demain, A.L., 2014. Importance of microbial natural products and the need to revitalize their discovery. *Journal of industrial microbiology and biotechnology*, 41(2), pp.185-201.
16. Diale, M. O., Kayitesi, E., and Serepa-Dlamini, M. H. (2021). Genome in silico and in vitro analysis of the probiotic properties of a bacterial endophyte, *Bacillus paranthracis* strain MHSD3. *Front. Genet.* 12:672149. doi: 10.3389/fgene.2021.672149
17. Dubey, M.K., Meena, M., Aamir, M., Zehra, A. and Upadhyay, R.S., 2019. Regulation and role of metal ions in secondary metabolite production by microorganisms. In *New and future developments in microbial biotechnology and bioengineering* (pp. 259-277). Elsevier.
18. Dührkop, K., Fleischauer, M., Ludwig, M., Aksenov, A.A., Melnik, A.V., Meusel, M., Dorrestein, P.C., Rousu, J. and Böcker, S., 2019. SIRIUS 4: a rapid tool for turning tandem mass spectra into metabolite structure information. *Nature methods*, 16(4), pp.299-302.
19. Dührkop, K., Shen, H., Meusel, M., Rousu, J. and Böcker, S., 2015. Searching molecular structure databases with tandem mass spectra using CSI: FingerID. *Proceedings of the National Academy of Sciences*, 112(41), pp.12580-12585.
20. Ezelarab, H. A., Hassan, H. A., Abuo-Rahma, G. E. D. A., and Abbas, S. H. (2023). Design, synthesis, and biological investigation of quinoline/ciprofloxacin hybrids as antimicrobial and anti-proliferative agents. *J. Iran. Chem. Soc.* 20, 683–700. doi: 10.1007/s13738-022-02704-7.
21. Hameed, I.H., Cotos, M.R.C. and Hadi, M.Y., 2017. A review: *Solanum nigrum* L. antimicrobial, antioxidant properties, hepatoprotective effects and analysis of bioactive natural compounds. *Research Journal of Pharmacy and Technology*, 10(11), pp.4063-4068.
22. Hoffmann, M.A., Nothias, L.F., Ludwig, M., Fleischauer, M., Gentry, E.C., Witting, M., Dorrestein, P.C., Dührkop, K. and Böcker, S., 2021. Assigning confidence to structural annotations from mass spectra with COSMIC. *BioRxiv*, pp.2021-03.
23. Jiang, Q., 2014. Natural forms of vitamin E: metabolism, antioxidant, and anti-inflammatory activities and their role in disease prevention and therapy. *Free Radical Biology and Medicine*, 72, pp.76-90.
24. Kannan, M., Kumar, T.S. and Rao, M.V., 2016. Antidiabetic and antioxidant properties of *Waltheria indica* L., an ethnomedicinal plant. *International Journal of Pharma Research and Health Sciences*, 4(5), pp.1376-1384.
25. Kaur, N., Arora, D.S., Kalia, N. and Kaur, M., 2020. Bioactive potential of endophytic fungus *Chaetomium globosum* and GC–MS analysis of its responsible components. *Scientific Reports*, 10(1), p.18792
26. Khare, S.K., Kumar, A. and Kuo, T.M., 2009. Lipase-catalyzed production of a bioactive fatty amide derivative of 7, 10-dihydroxy-8 (E)-octadecenoic acid. *Bioresource technology*, 100(3), pp.1482-1485.
27. Kodoli, R. S., Galatage, S. T., Killedar, S. G., Pishwikar, S. A., Habbu, P. V., & Bhagwat, D. A. (2021). Hepatoprotective activity of *Phyllanthus niruri* Linn. endophytes. *Future Journal of Pharmaceutical Sciences*, 7(1), 97.
28. Kumar, S., Stecher, G., Li, M., Knyaz, C. and Tamura, K., 2018. MEGA X: molecular evolutionary genetics analysis across computing platforms. *Molecular biology and evolution*,
29. Lee, S.J. and Lim, K.T., 2006. 150 kDa glycoprotein isolated from *Solanum nigrum* Linne stimulates caspase-3 activation and reduces inducible nitric oxide production in HCT-116 cells. *Toxicology in vitro*, 20(7), pp.1088-1097.
30. Liu, L. Y., Yang, Y. K., Wang, J. N., & Ren, J. G. (2022). Steroidal alkaloids from *Solanum nigrum* and their cytotoxic activities. *Phytochemistry*, 202, 113317.
31. Masood A., Khan M.A., Ahmad I., Breena E., Raza A., Ullah F., Shah S.A.A. (2023). Synthesis, characterization, and biological evaluation of 2-(n-((2'-(2h-tetrazole-5-yl)-[1,1'-biphenyl]-4yl)-methyl)-pentanamido)-3-methyl butanoic acid derivatives. *J. Molec*, 28 (4), 1908.
32. Martins, N., Barros, L. and Ferreira, I.C., 2016. In vivo antioxidant activity of phenolic compounds: Facts and gaps. *Trends in Food Science & Technology*, 48, pp.1-12.

33. Madema, M.H., Paalvast, Y., Nguyen, D.D., Melnik, A., Dorrestein, P.C., Takano, E. and Breitling, R., 2014. Pep2Path: automated mass spectrometry-guided genome mining of peptidic natural products. *PLoS computational biology*, 10(9), p.e1003822.
34. McParland, E., Benitez-Nelson, C.R., Taylor, G.T., Thunell, R., Rollings, A. and Lorenzoni, L., 2015. Cycling of suspended particulate phosphorus in the redoxcline of the Cariaco Basin. *Marine Chemistry*, 176, pp.64-74.
35. McRose, D.L. and Newman, D.K., 2021. Redox-active antibiotics enhance phosphorus bioavailability. *Science*, 371(6533), pp.1033-1037.
36. Mohamad, O.A., Li, L., Ma, J.B., Hatab, S., Xu, L., Guo, J.W., Rasulov, B.A., Liu, Y.H., Hedlund, B.P. and Li, W.J., 2018. Evaluation of the antimicrobial activity of endophytic bacterial populations from Chinese traditional medicinal plant licorice and characterization of the bioactive secondary metabolites produced by *Bacillus atrophaeus* against *Verticillium dahliae*. *Frontiers in microbiology*, 9, p.924.
37. Molyneux, P., 2004. The use of the stable free radical diphenylpicrylhydrazyl (DPPH) for estimating antioxidant activity. *Songklanakarin J. sci. technol*, 26(2), pp.211-219.
38. Narayanan, Z. and Glick, B.R., 2022. Secondary metabolites produced by plant growth-promoting bacterial endophytes. *Microorganisms*, 10(10), p.2008.
39. Narkhede, A.N., Kasote, D.M., Kuvalekar, A.A., Harsulkar, A.M. and Jagtap, S.D., 2016. Amarkand: A comprehensive review on its ethnopharmacology, nutritional aspects, and taxonomy. *Journal of Intercultural Ethnopharmacology*, 5(2), p.198.
40. Numan, M., Shah, M., Asaf, S., Ur Rehman, N. and Al-Harrasi, A., 2022. Bioactive compounds from endophytic bacteria *Bacillus subtilis* strain EP1 with their antibacterial activities. *Metabolites*, 12(12), p.1228.
41. Osbourn A. (2010). Secondary metabolic gene clusters: evolutionary toolkits for chemical innovation. *Trends Genet.* 26, 449–457.
42. Pandey, S. S., Jain, R., Bhardwaj, P., Thakur, A., Kumari, M., Bhushan, S., & Kumar, S. (2022). Plant probiotics–endophytes pivotal to plant health. *Microbiological Research*, 263, 127148.
43. Pant, A., & Vasundhara, M. (2023). Endophytic fungi: a potential source for drugs against central nervous system disorders. *Brazilian Journal of Microbiology*, 54(3), 1479-1499.
44. Photolo, M. M., Mavumengwana, V., Sitole, L., & Tlou, M. G. (2020). Antimicrobial and antioxidant properties of a bacterial endophyte, *Methylobacterium radiotolerans* MAMP 4754, isolated from *Combretum erythrophyllum* seeds. *International Journal of microbiology*, 2020(1), 9483670.
45. Pawle G., Singh S.K., (2014). Antimicrobial, antioxidant activity and phytochemical analysis of an endophytic species of *Nigrospora* isolated from living fossil *Ginkgobiloba*. *Curr. Res. Environ. App. Mycol.* 4 (1), 1–9.
46. Qi, D., Zou, L., Zhou, D., Zhang, M., Wei, Y., Li, K., et al. (2022). Biocontrol potential and antifungal mechanism of a novel *Streptomyces sichuanensis* against *Fusarium oxysporum* f. sp. *cubense* tropical race 4 in vitro and in vivo. *Appl. Microbiol. Biotechnol.* 106, 1633–1649. doi: 10.1007/s00253-022-11788-3
47. Russo, C. A. D. M., & Selvatti, A. P. (2018). Bootstrap and rogue identification tests for phylogenetic analyses. *Molecular Biology and Evolution*, 35(9), 2327-2333.
48. Sathwara, R. P. (2016). Nature, Spectroscopy Applications and Biological Activities Triazoles. *Nature*.
49. Seixas, A.F., Quendera, A.P., Sousa, J.P., Silva, A.F., Arraiano, C.M. and Andrade, J.M., 2022. Bacterial response to oxidative stress and RNA oxidation. *Frontiers in Genetics*, 12, p.821535.
50. Shaikh S., Verma H., Yadav N., Jauhari M., Bullangowda J. (2012). Applications of steroid in clinical practice. *Rev. Plan.*, 12 (2), 313.
51. Sharma, V. and Sharma, K.V., 2010. Synthesis and Biological Activity of Some 3, 5-Diarylisoxazoline Derivatives: Reaction of Substituted Chalcones with Hydroxylamine Hydrochloride. *Journal of Chemistry*, 7(1), pp.203-209.
52. Sharma, P., Piyushbhai, M. K., Venkatachalam, K., & Binesh, A. (2024). Exploring the Role of Secondary Metabolites from Plants and Microbes as Modulators of Macrophage Differentiation. *Cardiovascular & Hematological Disorders-Drug Targets*.
53. Sharrar, A.M., Crits-Christoph, A., Méheust, R., Diamond, S., Starr, E.P. and Banfield, J.F., 2020. Bacterial secondary metabolite biosynthetic potential in soil varies with phylum, depth, and vegetation type. *MBio*, 11(3), pp.10-1128.
54. Stuart, M. C., Kouimtzis, M., and Hill, S. (2009). *WHO model formulary 2008*. Geneva: World Health Organization.
55. Rehman, S. and Khan, H., 2017. Advances in antioxidant potential of natural alkaloids. *Current Bioactive Compounds*, 13(2), pp.101-108.
56. Rojas-Aedo, J.F., Gil-Durán, C., Del-Cid, A., Valdés, N., Álamos, P., Vaca, I., García-Rico, R.O., Levicán, G., Tello, M. and Chávez, R., 2017. The biosynthetic gene cluster for andrastin A in *Penicillium roqueforti*. *Frontiers in Microbiology*, 8, p.813.
57. Taghavi, S., Barac, T., Greenberg, B., Borremans, B., Vangronsveld, J., & van der Lelie, D. (2005). Horizontal gene transfer to endogenous endophytic bacteria from poplar improves phytoremediation of toluene. *Applied and environmental microbiology*, 71(12), 8500-8505.
58. Tan, D., Ertunc, M.E., Konduri, S., Zhang, J., Pinto, A.M., Chu, Q., Kahn, B.B., Siegel, D. and Saghatelian, A., 2019. Discovery of FAHFA-containing triacylglycerols and their metabolic regulation. *Journal of the American Chemical Society*, 141(22), pp.8798-8806. Thompson, J.D., Higgins, D.G. and Gibson, T.J., 1994. CLUSTAL W: improving the sensitivity of progressive multiple sequence alignment through sequence weighting, position-specific gap penalties and weight matrix choice. *Nucleic acids research*, 22(22), pp.4673-4680.
59. Tiwari, P., & Bae, H. (2020). Horizontal gene transfer and endophytes: An implication for the acquisition of novel traits. *Plants*, 9(3), 305.

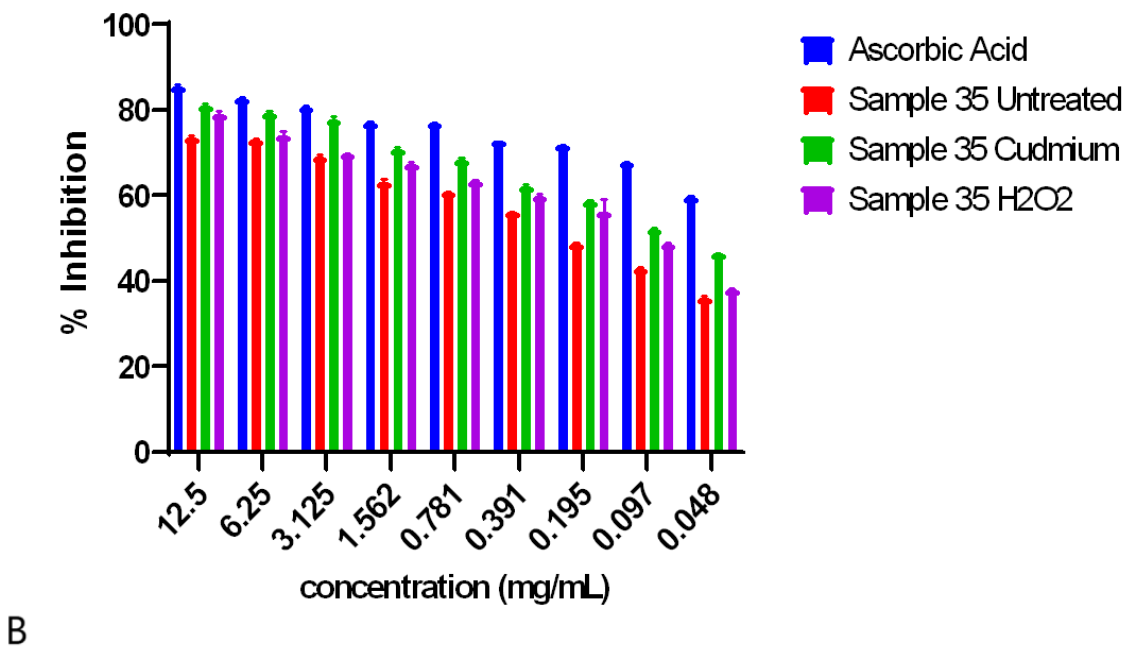
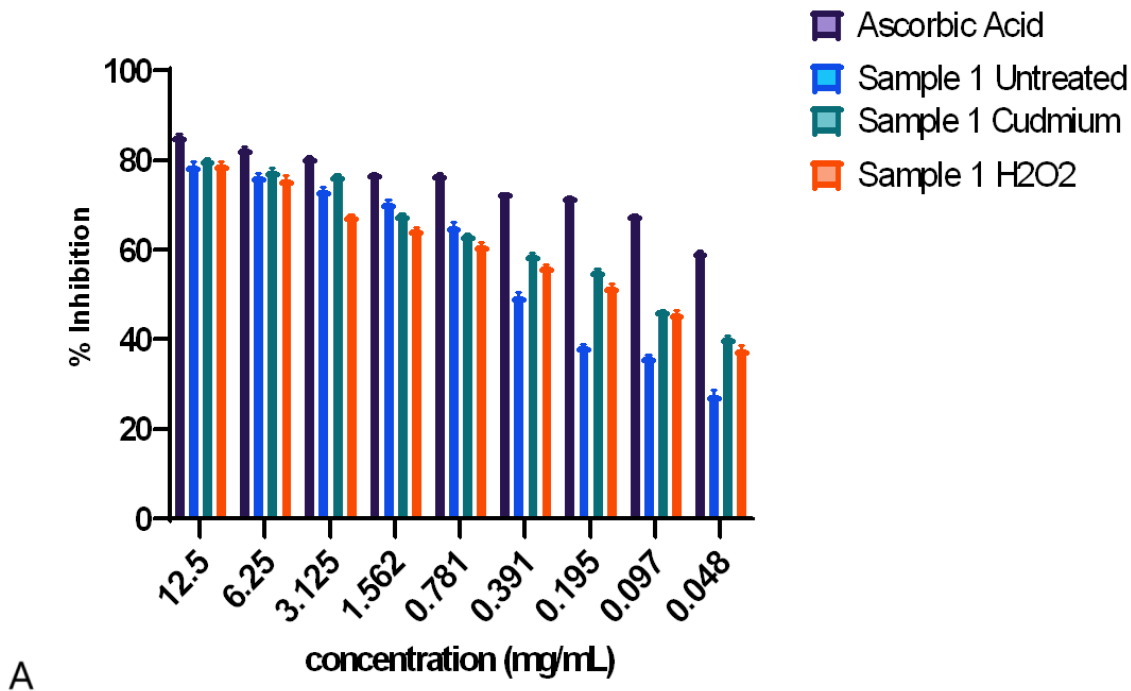
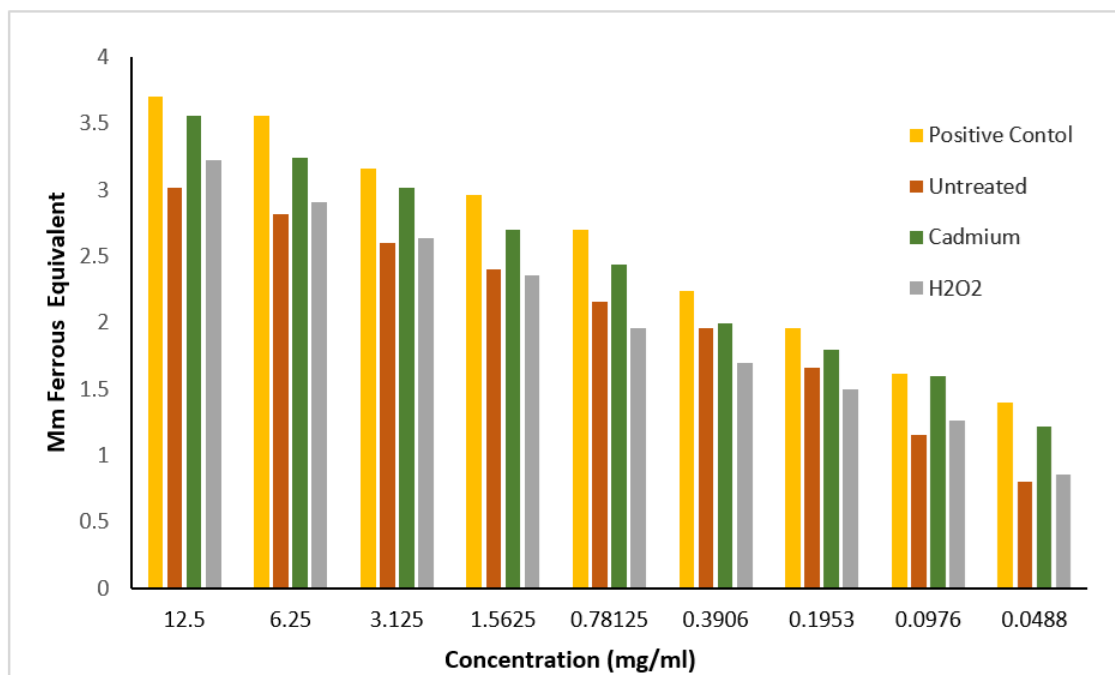


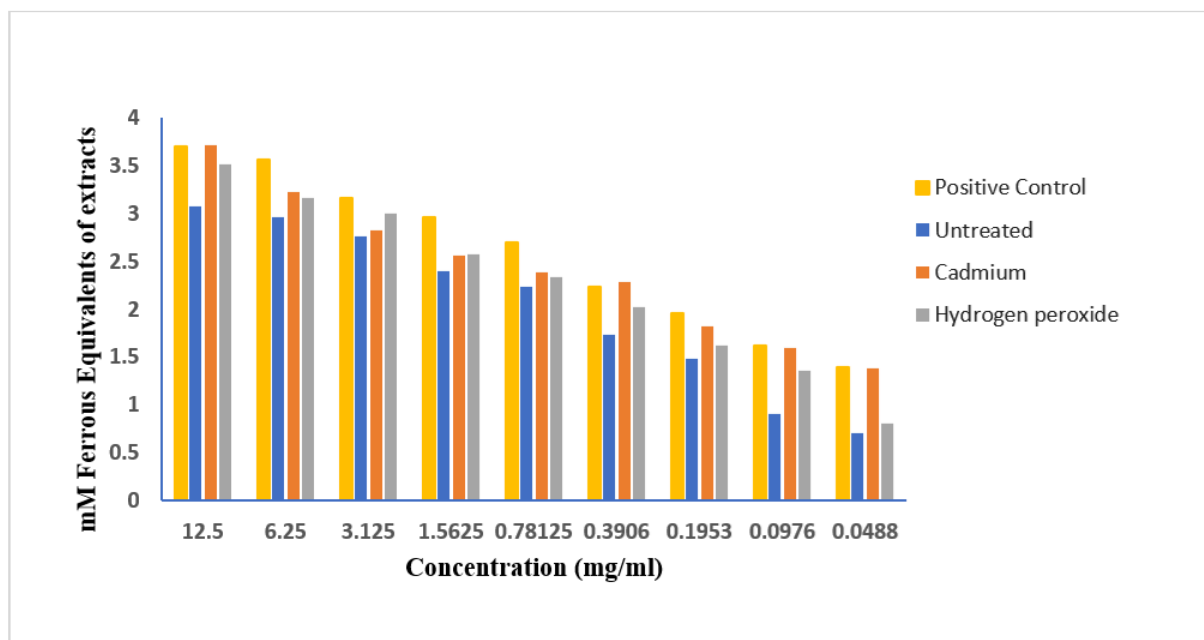
Figure 2

A: Figure 2B. DPPH free radical scavenging activity of *Bacillus* sp. NV1 methanolic crude extracts (n=3), p values less than 0.05 were statistically different. Vitamin C was used as a positive control.

B. DPPH free radical scavenging activity of *Bacillus* sp. NV35 methanolic crude extracts (n=3), p values less than 0.05 were statistically different. Vitamin C was used as a positive control.



A



B

Figure 3

A: Ferric reducing power of the methanolic *Bacillus* sp. NV1 crude extract. The Ferrous equivalents of crude extracts in (mM) versus the varying concentrations in (mg/ml). FRAP Positive control was used as positive reference to the crude extracts.

B: Ferric reducing power of the methanolic *Bacillus* sp. NV35 crude extract. The Ferrous equivalents of crude extracts in (mM) versus the varying concentrations in (mg/ml). FRAP Positive control was used as positive reference to the crude extract.